Spectral Broadening of Characteristic γ-Ray Emission Peaks from $^{12}C(^3He, p\gamma)^{14}N$ Reactions in Fusion Plasmas

M. Tardocchi,[1,2] M. Nocente,[2,1] I. Proverbio,[2] V. G. Kiptily,[3] P. Blanchard,[4] S. Conroy,[5] M. Fontanesi,[2] G. Grosso,[1] K. Kneupner,[3] E. Lerche,[6] A. Murari,[7] E. Perelli Cippo,[2] A. Pietropaolo,[2] B. Syme,[3] D. Van Eester,[6] and G. Gorini[2,1]

[1]*Istituto di Fisica del Plasma, EURATOM-ENEA-CNR Association, Milan, Italy*
[2]*Università degli Studi di Milano-Bicocca, Dipartimento di Fisica "G. Occhialini," Milan, Italy*
[3]*EURATOM-CCFE Association, Culham Science Centre, Abingdon, United Kingdom*
[4]*Centre de Recherches en Physique des Plasmas–CRPP, EPFL-SB, Lausanne, Switzerland*
[5]*EURATOM-VR, Department of Physics and Astronomy, Uppsala University, Uppsala, Sweden*
[6]*LPP-ERM/KMS, Association Euratom-"Belgian State," TEC Partner, B-1000, Brussels, Belgium*
[7]*Consorzio RFX, Padova, Italy*

(Received 2 May 2011; published 8 November 2011)

The spectral broadening of characteristic γ-ray emission peaks from the reaction $^{12}C(^3He, p\gamma)^{14}N$ was measured in $D(^3He)$ plasmas of the JET tokamak with ion cyclotron resonance heating tuned to the fundamental harmonic of ^3He. Intensities and detailed spectral shapes of γ-ray emission peaks were successfully reproduced using a physics model combining the kinetics of the reacting ions with a detailed description of the nuclear reaction differential cross sections for populating the $L1$-$L8$ ^{14}N excitation levels yielding the observed γ-ray emission. The results provide a paradigm, which leverages knowledge from areas of physics outside traditional plasma physics, for the development of nuclear radiation based methods for understanding and controlling fusion burning plasmas.

DOI: 10.1103/PhysRevLett.107.205002 PACS numbers: 52.70.La, 29.30.Kv, 52.55.Fa

Investigations of neutron and γ-ray emission from plasmas are motivated by the need to understand the nuclear processes occurring at the heart of a fusion burning experiment. Understanding and controlling the neutron emission at high power levels is the ultimate measure of the development of fusion research towards the goal of energy production. Fusion γ-ray emission rates are comparatively weaker but the role of γ rays as providers of information on the underlying fusion burning plasma state is emerging as a key asset. This is true for both inertial confinement fusion implosion experiments—where neutron and γ-ray emission can be used to understand the fusion reaction history, or measure fundamental parameters including the reacting fuel composition, ion temperature, ablator areal density, etc. [1–5]—and for magnetic confinement fusion—where neutron and γ-ray emission is expected to provide key information on the fusion burn conditions as well as on the physical processes involving α particles [6–14].

In order to develop neutron and γ-ray measurements in fusion burning plasmas the underlying physics must be discovered first. Even though the main reaction mechanisms may seem well identified, a lot remains to be done in order to unfold the underlying blend of plasma and nuclear physics. This task can be undertaken in present-day fusion experiments.

This Letter reports the first high-resolution investigation of γ-ray emission from a fusion plasma. The experiments were carried out on JET [15] under favorable experimental conditions such as large distance from the tokamak in a shielded low-background area, and interpreted using a model combining the kinetics of the reacting ions with a detailed description of the nuclear reaction differential cross sections and branching ratios for γ-ray emission.

The measurements were performed with a high purity germanium detector featuring 100% relative photopeak efficiency and 2.4 keV energy resolution at the calibration energy $E_\gamma = 1.33$ MeV [16]. Although commonly available at nuclear radiation laboratories, spectrometers of this kind were never used in fusion experiment. Operation in a present-day fusion environment was made possible by choosing N-type germanium, which is more resilient to neutron damage, and by equipping the detector with an electromechanical cooling system instead of liquid nitrogen cooling to facilitate operation in restricted areas. List mode digital acquisition recorded pulse height and time of each detection event; these data were converted to energy spectra after calibration with radiation sources providing <1 keV accuracy. The detector was placed in a shielded location 23 m above the tokamak viewing the plasma along a vertically collimated line of sight orthogonal to the toroidal magnetic field [17]. In these experiments the toroidal field value was 3.45 T and the plasma current ranged from 1.8 to 3.0 MA, which ensured good confinement of the fast ions. Ion cyclotron resonance heating (ICRH) was operated at a frequency of 33 MHz which is the fundamental resonance frequency of ^3He at the plasma axis major radius location of 2.84 m. Steady state ICRH power levels up to 6 MW were coupled to deuterium plasmas with electron densities of $2–3 \times 10^{19}$ m^{-3} and

electron and ion temperatures of $T_e \approx 3$-8 keV and $T_i \approx 3$-5 keV, respectively. The plasmas contained a moderate level of carbon and other impurities; ^{3}He minority concentration levels of 1%–5% were achieved after injecting small amounts of ^{3}He gas. These conditions are suitable for the generation of a population of energetic ^{3}He ions in the plasma in predominantly trapped orbits with velocities nearly perpendicular to the magnetic field. The presence of energetic ^{3}He ions was demonstrated by the γ-ray observations reported here.

A total of seven plasma discharges with several seconds of γ-ray emission were produced. Data collected from all discharges were added up to achieve good statistics in the γ-ray energy spectra. Evidence on energetic ^{3}He ions comes mainly from the two γ-ray spectral peaks at $E_{\gamma 1} = 2313$ keV and $E_{\gamma 2} = 1635$ keV shown in Fig. 1. Both peaks ride on top of a nearly flat background.

Statistical analysis of the $E_{\gamma 1}$ and $E_{\gamma 2}$ peaks after background subtraction yields intensities of $I_1 = 6516 \pm 80$ and $I_2 = 2755 \pm 53$ and peak widths—defined here as $W = 2.355\sigma$ where σ is the standard deviation—of $W_1 = 39.4 \pm 0.3$ keV and $W_2 = 26.5 \pm 0.4$ keV, respectively. For comparison the instrumental energy resolution is about 3.5 keV at these energies, which means that instrumental broadening of the peak shape is negligible. From the calculated HPGe photopeak efficiency and γ-ray attenuation along the viewing line the relative γ-ray yield is determined to be $r = Y_{\gamma 1}/Y_{\gamma 2} = 2.8 \pm 0.2$; the uncertainty is dominated by systematic error of photon transport simulations relating the plasma emissivity to the observed event rates. The analysis of the peaks and their shapes requires detailed knowledge of the underlying nuclear reaction differential cross sections and branching ratios for γ-ray emission. The ^{12}C(^{3}He, p)^{14}N* reaction is exothermic, with a Q value of 4.78 MeV, which exceeds the energy of the first two ^{14}N excitation levels. Level $L1$ at

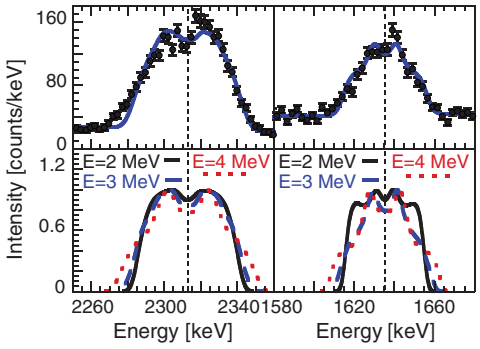

FIG. 1 (color). Top: experimental and fitted (solid line) peak shapes for the $E_{\gamma 1}$ (left) and $E_{\gamma 2}$ (right) γ-ray emission peaks. The unshifted $E_{\gamma 1} = 2313$ keV and $E_{\gamma 2} = 1635$ keV values are marked with vertical dashed lines. Bottom: Normalized simulated $E_{\gamma 1}$ (left) and $E_{\gamma 2}$ (right) peak shape for monoenergetic ^{3}He ions with Gaussian pitch angle distribution centered at $\theta_p = 90°$ and with FWHM = 10°.

2313 keV decays to the ground state with emission of $E_{\gamma 1}$ γ rays with $b_1 = 100\%$ probability (branching ratio). Level $L2$ at 3948 keV has a $b_2 = 96\%$ probability of decaying to level $L1$ thus emitting a cascade of $E_{\gamma 2}$ and $E_{\gamma 1}$ γ rays of equal intensities. At ^{3}He energies in the MeV range, ^{14}N excitation levels above $L2$ contribute to the peaks at $E_{\gamma 1}$ and $E_{\gamma 2}$ through cascade transitions as summarized in Table I. The effective cross section for emission of $E_{\gamma 1}$ and $E_{\gamma 2}$ γ rays is given by $\sigma_{\gamma 1} = \Sigma b_{i1} \cdot \sigma_{Li}$ and $\sigma_{\gamma 2} = \Sigma b_{i2} \cdot \sigma_{Li}$ where σ_{Li} ($i = 1$–8) is the cross section for populating the ith ^{14}N excitation level. These cross sections were determined from the differential cross section values available in the literature after some interpolation and consistency analysis [18]. All cross sections rise rapidly above 1 MeV and reach their largest values above 2 MeV. Main contributions to the $E_{\gamma 1}$ peak come from $L1$ and $L2$; however, contributions from the upper levels cannot be neglected. The situation is simpler for the $E_{\gamma 2}$ peak which is entirely due to $L2$ except for a resonance in the $L8$ cross section around $E_{3\mathrm{He}} = 3$ MeV. The relative γ-ray yield $r = \sigma_{\gamma 1}/\sigma_{\gamma 2}$ for monoenergetic ^{3}He is readily determined from the cross section values and is shown in Fig. 2. A detailed discussion of its wide oscillations in terms of the underlying nuclear structure properties is beyond the scope of the present work. The measured value $r = 2.8 \pm 0.2$ suggests that most of the γ-emitting ^{3}He ions in the plasma must have an energy below 3 MeV. One can go one step further and determine the yield ratio for the case of ^{3}He ions described by a Stix distribution with an asymptotic tail temperature $T_{3\mathrm{He}}$ (Fig. 2). The simulations show that the r value is only slightly sensitive to $T_{3\mathrm{He}}$ in the range 100 keV $< T_{3\mathrm{He}} <$ 500 keV. Any $T_{3\mathrm{He}}$ value within this range is compatible within the uncertainties of the measured r value.

The absolute level of the γ-ray count rate in the detector can be used to estimate the ^{3}He density $n_{3\mathrm{He}}$ in the plasma. The average rate at the $E_{\gamma 2} = 1635$ keV full energy peak was 98 ± 2 count/s, with a minimum and maximum value of 54 and 157 counts/s, respectively, during the seven discharges under analysis. This corresponds to an

TABLE I. Energies of the first eight ^{14}N excited states with branching ratios for emission of γ rays of energy $E_{\gamma 1} = 2313$ keV and $E_{\gamma 2} = 1635$ keV.

Level	Energy	b_1 (%)	b_2 (%)
$L1$	2313	100	0
$L2$	3948	96	96
$L3$	4915	0	0
$L4$	5106	20	1
$L5$	5691	64	0
$L6$	5834	16	1
$L7$	6204	77	0
$L8$	6446	21	19

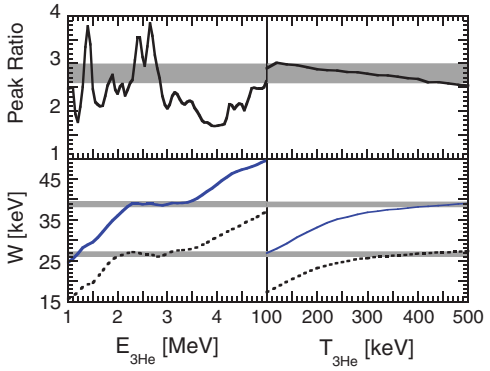

FIG. 2 (color). Peak ratio (top) and width (bottom) of the simulated $E_{\gamma 1}$ and $E_{\gamma 2}$ γ-ray emission peaks for monoenergetic ^{3}He ions of different energies (left) and Maxwellian ^{3}He ions of different temperatures (right). The horizontal bands are the experimental values.

estimated γ-ray emissivity of 1.7×10^{12} s^{-1} in the plasma core with systematic uncertainties of a factor 2 mainly due to the viewing line geometry. The emissivity changes significantly with the ^{3}He temperature with an increase of about 3 orders of magnitude as $T_{3\mathrm{He}}$ is raised from 200 to 500 keV. Assuming $T_{3\mathrm{He}} \approx 400$ keV and a ^{12}C density of 8.5×10^{-17} m^{-3} determined by CXRS data, the value $n_{3\mathrm{He}} = 6.8 \times 10^{17}$ m^{-3} is found. This is consistent with ^{3}He concentration values between 1% and 5% measured in real time during the discharges. Similar results are obtained by analyzing the $E_{\gamma 1} = 2313$ keV full energy peak.

We can now analyze the spectral broadening of the γ-ray peaks. The γ-ray energy in the lab system is Doppler shifted with respect to the reference value $E_{\gamma 0}$ by the amount $\Delta E_\gamma / E_{\gamma 0} = (V_N/c)\cos\theta_{\gamma N}$, where V_N is the ^{14}N* velocity and $\theta_{\gamma N}$ is the angle between the emitted γ ray and the excited ^{14}N* nucleus. In turn, the velocity of a γ ray is determined by simple kinematics from the initial ^{3}He velocity and the angle θ between the directions of the ^{3}He and the outgoing proton. Thus the final γ-ray energy spectrum reflects the energy and direction distribution of the initial ^{3}He population in the plasma, with weights provided by the differential cross section $d\sigma_i/d\Omega(\theta)$ ($i = 1$–8) for populating the $L1$-$L8$ ^{14}N levels.

The γ-ray spectrum is determined here using the Monte Carlo code GENESIS, a modified version of a code developed for neutron emission spectrometry applications [6]. An assumption made in the simulations is the absence of correlation in the γ-ray direction relative to the proton direction; i.e., each γ-ray emission direction with respect to the ^{14}N velocity is equally probable. This allows us to simulate the two reaction steps independently. Although the code can simulate the γ-ray spectrum from an extended ^{3}He distribution in the plasma volume, in this Letter we consider the simpler case of emission from a point in the plasma. Furthermore, we assume a Gaussian pitch angle distribution of the ^{3}He ions centered at $\theta_p = 90°$ and with FWHM $= 10°$; i.e., the ^{3}He ions gyrate with nearly perpendicular velocities around the horizontal magnetic field. Since the γ-ray spectrometry viewing line is also perpendicular to the magnetic field we expect the resulting γ-ray spectrum to be double humped. This is a well-known feature of fusion neutron, as well as proton, spectra for similar viewing geometries [19,20]. Examples of simulated γ-ray spectra for monoenergetic ^{3}He ions are shown in Fig. 1 for the $E_{\gamma 1}$ and $E_{\gamma 2}$ peaks and $E_{3\mathrm{He}} = 2$, 3, and 4 MeV. All spectra are symmetric around the unshifted energies $E_{\gamma 1}$ and $E_{\gamma 2}$ and do have a double hump shape though modulated by the angular dependence of the differential cross sections $d\sigma_i/d\Omega(\theta)$. To be noted is the spectral width. This is shown in Fig. 2 where the broadening $W = 2.355\sigma$ of the simulated γ-ray emission peaks is plotted for monoenergetic ions of energy up to 5 MeV. The peculiar behavior of the ^{12}C(^{3}He, $p\gamma$)^{14}N reaction cross sections results in a peak width that is practically independent of ^{3}He energy over the 2.0–3.5 MeV energy range. In the case of Maxwellian ^{3}He ion population of different temperature $T_{3\mathrm{He}}$ (Fig. 2), it is found that the broadening increases with the temperature. However, for $T_{3\mathrm{He}}$ values from 300 to 500 keV the variation is small (7%). Thus the experimental spectral width value is compatible with a broad range of $T_{3\mathrm{He}}$ values.

A similar conclusion is reached by detailed shape analysis of the γ-ray peaks. The simulated spectra fitted to the data in Fig. 1 assume ^{3}He ions described by a Stix distribution [21] with an asymptotic tail temperature $T_{3\mathrm{He}} = 400$ keV. The resulting reduced χ^2 values are $\chi^2 = 1.8$ for the $E_{\gamma 1}$ peak and $\chi^2 = 1.7$ for the $E_{\gamma 2}$ peak. The lower limit $T_{3\mathrm{He}}$ value resulting in a χ^2 increase by one is $T_{3\mathrm{He}} = 200$ keV. No useful upper limit to $T_{3\mathrm{He}}$ can be inferred: the simulated spectra shown in Fig. 3 feature a remarkable shape invariance above 300 keV. We conclude that a temperature value $T_{3\mathrm{He}} > 300$ keV was reached in the experiments reported here, $T_{3\mathrm{He}} \approx 400$ keV being a likely value based on the agreement between the expected γ-ray yield and the measured one for ^{3}He densities of a few percent and due to the minimum reduced χ^2 value obtained at this temperature.

Simulations of the rf heated ^{3}He energy distribution were performed with the CYRANO/TOMCAT wave codes [22,23]. The results indicate that temperatures above $T = 300$ keV were reached in all discharges, in agreement with the experimental evidence reported in this Letter.

When observed more carefully, the measured spectra in Fig. 1 seem to have an asymmetry in the top part of the spectrum: a few data points on the high energy side are systematically above the fitted curve whereas a few data points on the low energy side are systematically below the fitted curve. Our present model cannot account for the asymmetry, which is at the limit of statistical significance. Should better data confirm the evidence of asymmetry, a possible explanation can be sought by taking into account

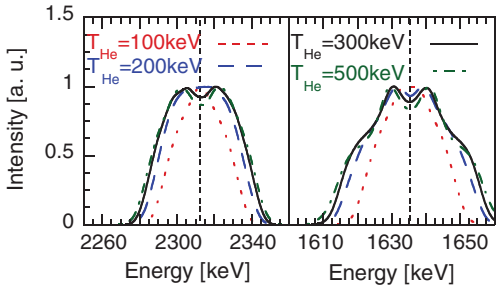

FIG. 3 (color). Simulated $E_{\gamma 1}$ (left) and $E_{\gamma 2}$ (right) γ-ray emission peak shapes normalized to unit height for ^{3}He ions described by a Stix distribution with several asymptotic tail temperatures $T_{3\mathrm{He}}$. The unshifted $E_{\gamma 1} = 2313$ keV and $E_{\gamma 1} = 1635$ keV values are marked with vertical dashed lines.

the viewing geometry and how it affects the full observation of gyration orbits around the magnetic field. Indeed we can reproduce the observed asymmetry if we assume that a $\sim$10% fraction of the gyrating ions falls out of the volume viewed by the spectrometer when moving downwards (i.e., away from the spectrometer). Evidence for effects of this kind can be sought, e.g., by looking for correlation with the ion orbit size: i.e., larger ion orbits should result in a stronger asymmetry in the gamma ray emission spectrum.

Another feature which seems to be marginally outside the statistical uncertainty and not accounted for by our model is an excess of events in the low energy side of the $E_{\gamma 1}$ peak. Peaks from the ^{3}He(^{9}Be, $p\gamma$)^{11}B reaction were also observed in the collected γ ray spectrum, but with lower intensities with respect to those from ^{3}He(^{12}C, $p\gamma$)^{14}N. Transitions from ^{11}B* excited states are expected to yield gamma rays of energies 2298 and 2265 keV, i.e., in the region where the excess of events for the $E_{\gamma 1}$ peak is observed. A detailed Monte Carlo simulation has not been done for this particular reaction, but we speculate that emission from ^{11}B* may be the reason of the observed excess of counts in the low energy side for the $E_{\gamma 1}$ peak. Because of this unaccounted component only the right-hand side ($E > E_{\gamma 1} = 2313$ keV) of the $E_{\gamma 1}$ peak was used to determine W_1 and χ^2 values.

In conclusion, high-resolution investigations of γ-ray emission from $D(^3\mathrm{He})$ fusion plasmas of the JET tokamak were reported. Intensities and detailed spectral shapes of γ-ray emission peaks from the reaction ^{12}C(^{3}He, $p\gamma$)^{14}N were successfully reproduced using a physics model combining the kinetics of the reacting ions accelerated by radio frequency waves in the plasma with a detailed description of the nuclear reaction differential cross sections $d\sigma_i/d\Omega(\theta)$ ($i = 1$–8) for populating the $L1$-$L8$ ^{14}N excitation levels yielding the observed γ-ray emission. The results represent a step forward in, and provide a paradigm for, the development of nuclear radiation based methods for understanding and controlling fusion burning plasmas.

This work was supported by EURATOM and carried out within the framework of the European Fusion Development Agreement. The views and opinions expressed herein do not necessarily reflect those of the European Commission. This work was done under the JET-EFDA workprogramme [24].

[1] J. A. Frenje *et al.*, Phys. Plasmas **17**, 056311 (2010).
[2] M. D. Cable *et al.*, Phys. Rev. Lett. **73**, 2316 (1994).
[3] H. W. Herrmann *et al.*, Rev. Sci. Instrum. **81**, 10D333 (2010).
[4] A. M. McEvoy *et al.*, Rev. Sci. Instrum. **81**, 10D322 (2010).
[5] N. M. Hoffmann *et al.*, Rev. Sci. Instrum. **81**, 10D332 (2010).
[6] L. Ballabio, G. Gorini, and J. Källne, Phys. Rev. E **55**, 3358 (1997).
[7] M. Nocente, G. Gorini, J. Källne, and M. Tardocchi, Nucl. Fusion **51**, 063011 (2011).
[8] J. Källne, L. Ballabio, J. Frenje, S. Conroy, G. Ericsson, M. Tardocchi, E. Traneus, and G. Gorini, Phys. Rev. Lett. **85**, 1246 (2000).
[9] L. Giacomelli *et al.*, Nucl. Fusion **45**, 1191 (2005).
[10] F. E. Cecil and D. E. Newman, Nucl. Instrum. Methods Phys. Res. **221**, 449 (1984).
[11] V. G. Kiptily, F. E. Cecil, and S. S. Medley, Plasma Phys. Controlled Fusion **48**, R59 (2006).
[12] W. W. Heidbrink and G. J. Sadler, Nucl. Fusion **34**, 535 (1994).
[13] W. W. Heidbrink, Phys. Plasmas **15**, 055501 (2008).
[14] B. N. Breizman and S. E. Sharapov, Plasma Phys. Controlled Fusion **53**, 054001 (2011).
[15] M. Keilhacker, A. Gibson, C. Gormezano, and P. H. Rebut, Nucl. Fusion **41**, 1925 (2001).
[16] I. L. Proverbio, Ph.D. thesis, Milano-Bicocca University, Italy, 2009.
[17] M. Gatu Johnson *et al.*, Plasma Phys. Controlled Fusion **52**, 085002 (2010).
[18] I. Proverbio, M. Nocente, V. G. Kiptily, M. Tardocchi, and G. Gorini, Rev. Sci. Instrum. **81**, 10D320 (2010).
[19] M. Tardocchi, S. Conroy, G. Ericsson, G. Gorini, H. Henriksson, and J. Källne, Nucl. Fusion **42**, 1273 (2002).
[20] W. W. Heidbrink, Nucl. Fusion **24**, 636 (1984).
[21] T. H. Stix, Nucl. Fusion **15**, 737 (1975).
[22] D. Van Eester and R. Koch, Plasma Phys. Controlled Fusion **40**, 1949 (1998).
[23] P. U. Lamalle, Plasma Phys. Controlled Fusion **40**, 465 (1998).
[24] F. Romanelli *et al.*, in *Proceedings of the 22nd Fusion Energy Conference, Geneva, Switzerland, 2008* [International Atomic Energy Agency (IAEA), Vienna, 2008]. (All the members of the JET-EFDA Collaboration appear in the appendix of this paper.)